

Fission fragment mass distribution studies in $^{32}\text{S}+^{197}\text{Au}$ and $^{36}\text{S}+^{197}\text{Au}$ reactions.

Shiva Prasad Nayak* and E. Prasad

Department of Physics, Central University of Kerala, Tejaswini hills, Periyar.

1. Introduction

The sun and other stars in the universe are powered by a process called nuclear fusion. Fusion becomes increasingly complicated when the interacting nuclei become heavier. Though fusion is characterised by the formation of the compound nucleus (CN), the probability of this CN formation drops down drastically with the increasing size of the colliding nuclei. The reseparation after the capture happens with larger probability leading to non-equilibrium processes, introducing severe suppression to fusion. The products separated before the CN formation appear fission-like (and hence called quasifission) and overlap significantly with fusion-fission products. Fusion suppression on the other hand makes the synthesis of new (artificial) elements very challenging. It is of great interest to know the extent of fusion suppression in heavy ion fusion, case by case, as fusion is a highly entrance channel dependent process. The role of neutrons along the isotopic chain of a given element in fusion/fusion suppression is also important. We here report the fusion measurements of $^{32,36}\text{S}+^{197}\text{Au}$ reactions forming the composite system $^{229,233}\text{Am}$. The fission/fission-like fragments are measured in this experiment.

2. Experimental Method

This experiments were carried out in the Heavy Ion Accelerator Facility of Australian National University (ANU) using the 14 UD pelletron accelerator and the superconducting linear accelerator (LINAC). Fission fragments were detected using the CUBE de-

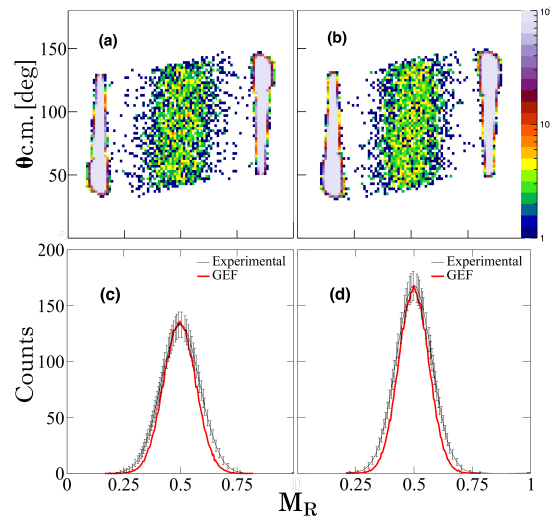


FIG. 1: See the text for details.

tector system [1]. Measurements have been performed for the ^{32}S and ^{36}S beams excitation energy ranging from 38-48 MeV and 29-41 MeV respectively with target ^{197}Au . The position and timing information from the MWPC detectors were used for obtaining the mass-angle distribution and mass-ratio distributions. Kinematic re-construction [2, 3] method has been used here.

3. Results

Mass angle distribution (MAD) for the $^{32}\text{S}+^{197}\text{Au}$ and $^{36}\text{S}+^{197}\text{Au}$ at $E/V_b = 1$ are shown in Fig. 1 (a) and (b) where E is center-of-mass energy and V_b is capture barrier [4], for example. Corresponding mass-ratio (M_R) distribution is shown in the bottom panels (c) and (d). The Gaussian fit to the experimental data (black curve) and theoretical calculations using GEF [5] (red curve) are also shown in the panels (c) and (d). A broadening of the experimental M_R distribution with respect to the GEF distribution is observed at all energies.

*Electronic address: nayakshiva011.spn@gmail.com

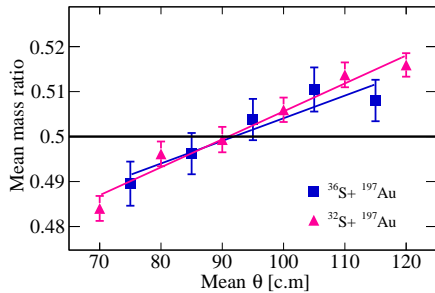


FIG. 2: Mean mass ratio as a function of mean angle for the two reactions. A slope indicates mass-angle correlation.

Experimental MADs are direct representation of the reaction outcome. In order to check possible mass-angle correlation, the MAD is sliced into smaller angular bins and the mean mass ratio is plotted. This is shown in Fig. 2 for both reactions at $E/V_b = 0.95$ for $^{32}\text{S}+^{197}\text{Au}$ and $E/V_b = 1$ for $^{36}\text{S}+^{197}\text{Au}$. The horizontal line (black) at $M_R = 0.5$ shows the case when there is no correlation. A clear mass-angle correlation is observed in both reactions at all energies. This correlation and the broadening of M_R distribution indicate the presence of quasifission in $^{32}\text{S}+^{197}\text{Au}$ and $^{36}\text{S}+^{197}\text{Au}$ reactions.

The widths (standard deviations from the Gaussian fit, σ) of the experimental M_R distributions are shown in Fig. 3 for the two reactions along with the theoretical estimates from GEF. A clear difference may be noticed in both reactions, from the theoretical estimates. From the experimental and theoretical mass widths, we have also estimated the probability for quasifission as well as fusion probability. It is noticed that the fusion probability ranges between 80–88 percentage in both reactions, in the measured energy range. No quasifission is observed in $^{16}\text{O} + ^{197}\text{Au}$ [6].

We next compare the systematics of fission/fission-like fragment mass widths in reactions using ^{197}Au as target which is shown in Fig. 4. An increase in mass width with increase in $Z_P Z_T$ is visible from Fig. 4, showing the dominance of quasifission when system become heavier. Except $^{16}\text{O} + ^{197}\text{Au}$, all other reaction exhibit signature of quasifission [6].

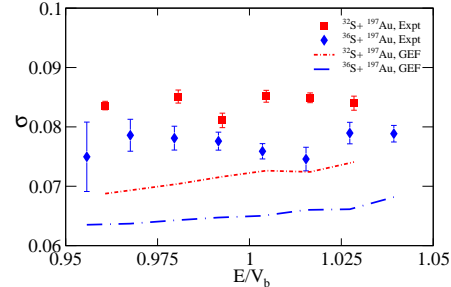


FIG. 3: Experimental σ for the two reactions are compared with GEF calculations.

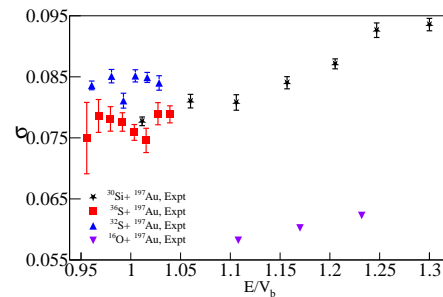


FIG. 4: Comparison of mass width of other reaction using ^{197}Au as target.

We also note larger mass width for the lighter (^{229}Am) isotope of Americium populated compared to the heavier one (^{233}Am). We are exploring possible role of neutron excess in this observation.

Acknowledgments

Authors acknowledge Prof. D. J. Hinde, Prof. M. Dasgupta and the entire nuclear physics team of Australian National University, Canberra for the support during the experiment.

References

- [1] N. R. Lobanov, Phys. Rev. Accel. Beams, 19, 072801 (2016).
- [2] D. J. Hinde et al., Phys. Rev. C53, 1290–1300 (1996).
- [3] J. Toke et al., Nucl. Phys. A440, 327–365 (1985).
- [4] W. J. Swiatecki et al., Phys. Rev. C71, 014602 (2005).
- [5] K.-H. Schmidt et al., Nuclear Data Sheets 131, 107 (2016).
- [6] S. Appannababu et al., Phys. Rev. C80, 024603 (2009).